



Prepared in cooperation with the U.S. Department of Energy Office of Environmental Management, National Nuclear Security Administration, Nevada Site Office, under Interagency Agreement Department of Energy Agreement DOE DE-AI52-07NA28100

A Refined Characterization of the Alluvial Geology of Yucca Flat and Its Effect on Bulk Hydraulic Conductivity

By G.A. Phelps, A. Boucher, and K.J. Halford

Open-File Report 2010-1307

U.S. Department of the Interior
U.S. Geological Survey

U.S. Department of the Interior
KEN SALAZAR, Secretary

U.S. Geological Survey
Marcia K. McNutt, Director

U.S. Geological Survey, Reston, Virginia: 2011

For product and ordering information:
World Wide Web: <http://www.usgs.gov/pubprod>
Telephone: 1-888-ASK-USGS

For more information on the USGS—the Federal source for science about the Earth,
its natural and living resources, natural hazards, and the environment:
World Wide Web: <http://www.usgs.gov>
Telephone: 1-888-ASK-USGS

Suggested citation:
Phelps, G.A., Boucher, A., and Halford, K.J., 2011, A refined characterization of the
alluvial geology of yucca flat and its effect on bulk hydraulic conductivity, U.S. Geological
Survey Open-File Report 2010-1307, 33 p. [<http://pubs.usgs.gov/of/2010/1307/>].

Any use of trade, product, or firm names is for descriptive purposes only and does not imply
endorsement by the U.S. Government.

Although this report is in the public domain, permission must be secured from the individual
copyright owners to reproduce any copyrighted material contained within this report.

Contents

Abstract	1
Introduction	1
Methods	3
Overview	3
Exploratory Data Analysis	5
Location of the Drill-Hole Data within the Study Area	5
Distribution of the Thickness of Facies	6
Spatial Structure	7
Models of the Alluvium	8
Overview	8
Sequential Indicator Simulation Models	9
Single Normal Equation Simulation models	10
Comparing the Models	12
Results and Discussion	13
Summary of Results	14
Acknowledgments	14
References	15
Figures	17

This page intentionally left blank

A Refined Characterization of the Alluvial Geology of Yucca Flat And Its Effect on Bulk Hydraulic Conductivity

G.A. Phelps¹, A. Boucher², and K.J. Halford³

Abstract

In Yucca Flat, on the Nevada National Security Site in southern Nevada, the migration of radionuclides from tests located in the alluvial deposits into the Paleozoic carbonate aquifer involves passage through a thick, heterogeneous section of late Tertiary and Quaternary alluvial sediments. An understanding of the lateral and vertical changes in the material properties of the alluvial sediments will aid in the further development of the hydrogeologic framework and the delineation of hydrostratigraphic units and hydraulic properties required for simulating groundwater flow in the Yucca Flat area. Previously published geologic models for the alluvial sediments within Yucca Flat are based on extensive examination and categorization of drill-hole data, combined with a simple, data-driven interpolation scheme. The U.S. Geological Survey, in collaboration with Stanford University, is researching improvements to the modeling of the alluvial section, incorporating prior knowledge of geologic structure into the interpolation method and estimating the uncertainty of the modeled hydrogeologic units.

Introduction

Yucca Flat is an extensional basin in the northeast corner of the Nevada National Security Site, Nye County, Nevada (fig. 1). The basin formed during the Tertiary as a result of eastward extension, and it is dominated by north-trending normal faults (Carr, 1984; Cole and Dickinson, 1987). Paleozoic and Precambrian sedimentary rocks form the basement of Yucca Flat Basin (Cole and others, 1997). Within the basin, a thin section of Eocene sedimentary deposits are overlain by a thick sequence of middle Miocene volcanic flows and tuffs erupted from sources in the southwestern Nevada volcanic field (Sawyer and others, 1994). Total thickness of the unconsolidated and partially consolidated alluvial and volcanic deposits exceeds 1 km in the deepest parts of the basin. At the surface, the alluvial deposits are formed from coalescing alluvial fans at the base of the mountains surrounding Yucca Flat. Drill-hole and tunnel data within Yucca Flat (Sweetkind and Drake, 2007; S. Drellack, written commun., 2007) indicate that the alluvial fans have been building in Yucca Flat since the cessation of volcanism during the late Miocene.

At the surface the alluvial material is composed of accumulations of sediments formed by debris flows and stream flows, much of which has been subsequently altered by processes that contribute to soil development. The resulting geomorphic units are mapped at the surface as separate Quaternary geologic units (Slate and others, 2000). In general, soil development increases with age. Older Quaternary geologic units that have well-developed soils have a larger mean clast size and a broader variance of particle-size

¹ U.S. Geological Survey, Menlo Park, Calif.

² Dept of Environmental Earth System Science, Stanford University, now at Advanced Resources and Risk Technology, LLC

³ U.S. Geological Survey, Carson City, Nev.

distribution than units with poorly developed soils, including higher percentages of silt and clay concentrated in layers centimeters to decimeters below the surface (Nimmo and others, 2009b). Consequently, older Quaternary geologic units generally have a lower hydraulic conductivity than younger units. Hydraulic conductivity can decrease by up to three orders of magnitude from the youngest Holocene soils to the oldest Pleistocene soils (Nimmo and others, 2009a).

The alluvial sediments that make up Yucca Flat Basin are composed of hydrologically diverse geologic units that were deposited through time as the basin filled. Thus, the often thick package of alluvial sediments that fills Yucca Flat is composed of layered, interfingering, geologic units of potentially very different hydraulic conductivity. The heterogeneous nature of the sediments potentially could impact predictions of saturated and unsaturated groundwater flow and contaminant transport within the basin.

In the subsurface the flow of groundwater through the alluvium depends on the location of hydrologically heterogeneous alluvial geologic units. At the surface these units can be mapped, but at depth their configuration must be estimated from drill-hole information and deterministic or statistical models. It is these deterministic or statistical models, therefore, that govern the bulk hydraulic characteristics of the alluvium that is used in hydrologic models.

Most current hydrologic models of the alluvium in Yucca Flat assume that the sediments are homogeneous and that their hydraulic conductivity is a simple function that, due to the effects of compaction, decreases with depth (Belcher and others, 2004). This model of the alluvium in the subsurface is referred to as the “homogeneous model” for the rest of this paper. Sweetkind and Drake (2007) used commercially available software to generate a deterministic model of the alluvial sediments within Yucca Flat. The authors define 12 discrete geologic units, primarily based on descriptions of particle size from drill holes, and they use these data as the foundation of the alluvial model. In their model, every location is assigned a geologic unit equivalent to that observed in the nearest neighboring drill hole (from here on referred to as the “nearest neighbor model”). These models are the only models currently available that describe spatial variations in the alluvial sediment within Yucca Flat, and each omits data dependencies seen in the surface geology and the drill-hole data, resulting in models that lack the spatial structure observed in alluvial units in outcrop and on geologic maps. Furthermore, because each model is deterministic it provides only a single estimate of the sediment’s hydrologic properties.

Previous work suggests hydrologic flow models can be sensitive to the configuration of subsurface geologic units. Estimates of hydraulic conductivity and flow and transport through the alluvial units in the subsurface, at least at the outcrop scale, are affected by facies changes in alluvial sediments (Guertel and others, 1994; Klise and others, 2009).

This report uses existing data, the drill-hole data as categorized by Sweetkind and Drake (2007), to generate geostatistical models of a rectangular volume of alluvium within Yucca Flat. Two geostatistical methods are used in this report to generate suites of models (each individual model in the suite is called a “realization”) of the alluvium beneath Yucca Flat. Each geostatistical method generates a suite of realizations that, when taken together, model the alluvium. The suite of realizations replaces the notion of a single model; no single realization is “better” than another, they are all equally probable

given the geostatistical specifications. Together the realizations represent a group of possible geologic alternatives, as opposed to the homogeneous or nearest neighbor model, where a single model specifies the subsurface alluvium. Additionally, for a suite of realizations, uncertainty due to variation within the alluvium can also be characterized by the variation among individual realizations. The previous models cannot characterize such uncertainty because each consists of only a single, deterministic model, rather than multiple realizations, each representing one possible configuration of the geology in the subsurface.

The new models, generated using the geostatistical methods, are compared to previous models by a simple test—measuring the saturated bulk hydraulic conductivity for a rectangular volume of alluvial sediments within the basin. More sophisticated comparisons of the modeling methods are beyond the scope of this report, but would be a natural continuation of the investigation.

To avoid confusion about the use of the term “model,” suites of realizations generated by a particular geostatistical method and set of parameters will be referred to as a particular geostatistical model, and the individual realizations generated using that method and parameters (which could also be thought of as individual models) will be referred to as realizations.

Methods

Overview

The alluvium in Yucca Flat was evaluated by building upon previous geologic mapping (Slate and others, 2000) and drill-hole studies (Sweetkind and Drake, 2007). Slate and others (2000) mapped four Quaternary geologic units at the surface in Yucca Flat Basin (fig. 2). Sweetkind and Drake (2007) divided the sediment record from 285 drill holes (17,291 m of drill-hole data) out of approximately 900, that most completely describe the alluvial section in Yucca Flat (fig. 3) into facies based primarily on particle size, and secondarily on lithology (table 1). Statistical properties of the sediments were analyzed using the geologic units from the map and facies defined by Sweetkind and Drake (2007). Geologic map data were used for spatial pattern analysis, as is discussed in the section titled Models. Drill-hole facies, as defined by Sweetkind and Drake (2007), are discussed throughout the remainder of this section. These facies were examined for any potential trends describing the three dimensional nature of the alluvium. Minor facies, such as basalt and limestone, lack sufficient drill-hole data to be characterized statistically and were omitted from the statistical portion of the analysis. These remaining facies (the first seven facies listed in table 1) represent particle size distributions, from fine to coarse, and are the subject of further discussion.

Table 1. Thickness statistics for alluvial units as defined by Sweetkind and Drake, 2007.				
alluvial unit	total thickness (m)	thickness, 1st quartile (m)	thickness, median (m)	thickness, 3rd quartile (m)
gravel	1,875	3	14	55
sandy gravel	15,536	15	91	163
gravelly sand	21,598	15	64	150
sand and minor gravel	16,970	9	38	102
sand clay and gravel	2,740	46	133	201
coarse sand	8,766	8	21	63
fine sand	1,114	3	11	37
clay	74	*	*	*
clay and sand	712	*	*	*
clay and limestone	93	*	*	*
basalt	96	*+	*+	*+
nonwelded tuff	91	*+	*+	*+
*units too limited in occurrence to characterize statistically.				
+these units are not alluvial, but were encountered within the alluvial section in drill holes.				

The drill-hole data were first checked for consistency, ensuring that adjacent facies of the same type were combined, and that all lengths of missing records were coded properly as “nodata.” Only facies present in sufficient amounts (the first seven facies in table 1) and with ample drill-hole data were characterized statistically.

Exploratory data analysis was used to identify potential non-spatial and spatial trends in the data. The exploration process graphically compared unit type and thickness to depth of occurrence, distance from the edges of the basin, gravitational anomaly (a surrogate for basin depth), and gravitational gradient (a surrogate for basin gradient and response to tectonic activity). The graphs were inspected visually for trends in the data. The spatial distribution of facies within the basin was analyzed to determine if strong trends existed in the distribution of coarse-grained versus fine-grained facies. The analysis, detailed in the next section, revealed only minor trends in the data.

After the spatial trends were assessed, three geostatistical models were generated based on the measured spatial properties. Each geostatistical model contains a set of statistical parameters that define the characteristics of the model. From these characteristics, many individual geologic realizations can be created, each slightly different, but having the same general tendencies as set by the specified statistical parameters.

The first geostatistical model is based on spatial continuity of 1 km, the second is based on spatial continuity of 4 km, and the third is based on the spatial patterns quantitatively derived from the geologic map. For each geostatistical model, 25 realizations of the possible configuration of alluvium in the subsurface are generated. Once the realizations were generated, their bulk hydraulic conductivity was compared as a simple test of the differences between the geostatistical models.

Exploratory Data Analysis

The goal of exploratory data analysis of the drill-hole data was to identify any potential non-spatial and spatial trends in the subsurface occurrence and thickness of the facies in table 1. This was accomplished by graphical inspection. The exploratory process required investigating the statistical distribution of occurrence and thickness of each facies, and any potential trends with compass direction, depth, and autocorrelation. Additional analyses included examining facies occurrence and thickness as they relate to distance from the edges of the basin (a surrogate for distance from the sediment source), the gravitational anomaly over the basin (a surrogate for basin depth), and gravitational gradient (a surrogate for basin gradient and response to tectonic activity). Together these analyses are intended to highlight any patterns of sedimentation within the basin. Minor facies, those having a cumulative thickness of less than 1,000 m and limited drill-hole penetration (table 1), could not be characterized statistically and were not included in the exploratory analyses.

The drill-hole data exhibited significant spatial autocorrelation in the vertical direction. Although no significant trends were identified in the thickness of the facies, minor trends were noted that may indicate patterns in sedimentation through time. These minor trends are discussed in detail below.

Location of the Drill-Hole Data within the Study Area

The spatial sampling of the drill-hole data affects the analyses of facies distribution and thicknesses within Yucca Flat Basin. The characterization of the Yucca Flat alluvium presented in the following sections of the report is based on a sampling of irregularly-spaced drill holes drilled for multiple purposes over several decades. Because no consistent sampling design could be implemented for this analysis, the resolution of the sampled dataset can only be approximated from scattered drill-hole locations.

The horizontal resolution of the data set is determined by the distance between the drill holes. The location of the sampling throughout the study area determines the degree to which the samples are representative of the entire study area. The clustering of the sampling determines the scale of the structures that are resolvable throughout the basin. Together, the location and clustering provide a general guide to the horizontal resolution of the data set. Because data are obtained from drill holes, which sample the depth profile nearly continuously, the vertical resolution of the data set is much finer than the horizontal resolution and is most often less than 5 m.

The 285 drill holes used in the analysis are scattered throughout the basin. The densest clustering of the data occurs in the northern and central parts of the basin with the sparsest coverage occurring along the western and southern edges of the basin (fig. 3). Figure 4 shows the area within the basin, as a percentage, that is within a given distance of the nearest drill hole. The figure indicates that 60 percent of the area of the basin is within one km of the nearest drill hole, and that 95 percent of the area of the basin is within four km of the nearest drill hole. In other words, structures of one km or greater in size can be resolved over 60 percent of the basin, and structures of 4 km or greater in size can be resolved over 95 percent of the basin.

Spatial clustering of the drill-hole data can be measured by examining the distribution of the distance to natural neighbors of the sample locations (fig. 5). Natural

neighbors are points that share the edge of a Delaunay Triangle. Delaunay triangles are formed from a set of (scattered) points by ensuring that the circumscribing circle of any triangle (formed by connecting the points of the set by straight lines) does not contain a point (Laurini and Thompson, 1992). Figure 5 shows that 60 percent of the drill holes are within one km, and 90 percent of the drill holes are within two km, of their neighbors. This tight, even clustering is seen throughout the central portion of the basin in map view in figure 2. Therefore, in more than 60 percent of the basin, using 60 percent of the drill holes, features of 1 km or greater in horizontal length are resolvable.

Distribution of the Thickness of Facies

The purpose of the following analysis is to determine which alluvial facies are abundant and which are scarce, and whether there exists any pattern in the thickness distribution. The alluvial facies examined in this analysis represent a broad spectrum of clastic sediments, from coarse material composed of gravel to fine material composed of fine sand. The analysis highlights positive and negative results. Although no strong patterns were discovered, weak trends were identified.

The most abundant facies within the basin consist of mixed sand and gravel: sandy gravel, gravelly sand, sand and minor gravel. These facies make up 76 percent of the total thickness sampled.

With the exception of the “gravel” and “sand, clay and gravel” facies, the median thickness of the alluvial facies increases with increasing particle size (fig. 6). Box plots in figure 6 indicate that thickness increases nearly an order of magnitude, that the thickness distributions are skewed towards smaller thicknesses, and that mid-range particle sizes have a larger variability than the extremes of very coarse or very fine material. The thickness of each facies varies over an order of magnitude, generally from less than 1 m to more than 200 m.

To investigate possible trends in facies thickness, both laterally and with depth, the basin was separated into four quadrants (fig. 3) of roughly equal data density. The thickness and depth were compared in each quadrant, first ignoring facies differences (fig. 7), and then conditioning the data by facies. Figure 8 shows an example of a comparison of thickness distributions for lithologies occurring at a depth between 100 and 200 m. The depth used in the analysis is the base of the facies. Although the box plots indicate that the spread of the thickness of the facies tends to increase with depth, this increase is not a trend in the data, but rather is caused by limitations of the facies closer to the surface (for example, facies within 100 m of the surface cannot be thicker than 100 m, by definition). The analysis could not discern any clear trend in facies thickness with depth or laterally across the basin.

Geologic principles suggest relationships between facies thickness and distance from sediment source, depth of the tectonic basin, and gradient of the tectonic basin within Yucca Flat. Surrogates for each of these variables were used to investigate potential trends in the drill-hole data.

Facies thickness relative to the distance from the sediment source was approximated by using the distance from the edges of Yucca Flat Basin. This approximation is assumed reasonable considering that sediment sources must occur beyond the edge of the basin, and the deeper parts of the basin are, for the most part, farther from the basin edges. Figure 9 plots facies thickness against the distance from the edge of the Yucca Flat Basin for the four most abundant facies from the drill-hole data.

Moving averages, using the locally weighted regression method with a span of 0.5 (Cleveland, 1979), were used in an attempt to expose trends hidden in the scattered data. While the moving-average curves show a tendency to thin about three km from the edge of the basin, that trend reverses, and scatter again dominates the data. The coarse-sand curve shows a slight increase with distance from the edge of the basin, but no clear trend emerges from this analysis.

Facies thickness relative to the measured gravity anomaly (Ponce, 1997) was examined because the size of the gravitational anomaly correlates to the tectonic depth of the basin—the larger the gravitational anomaly, the deeper the basin. However, upon examination of figure 10, this relationship shows a similar scatter to that shown in the previous plot of distance from the basin edge (fig. 9). The moving-average curves show a tendency for the coarser facies to reach an average maximum thickness at about -20 mGal. To some extent, the location of the areas of average facies thinning, as indicated by the distance from the edge of the basin, and the location of the areas of average facies thickening as indicated by the isostatic residual gravity, overlap spatially within the basin; that is, correlations with the distance from the edge of the basin suggests units are thinning where correlations with the isostatic residual gravity suggests units are thickening. The two analyses appear to be contradicting one another. This contradiction, the scatter in the data, and the lack of a geologic explanation for any observed weak trend, casts doubt on the significance of each trend. The average tendencies of the thicknesses do not appear to describe meaningful trends in the data.

Finally, the gravitational gradient (measured in mGal/meter, normalized to 100) was used as a surrogate to represent the topographic gradient of the tectonic basin in Yucca Flat. Steeper slopes may have affected sediment thickness during basin formation. Once again, however, scatter in the data similar to that noted in previous plots (figs. 9 and 10) can be seen (fig. 11), and the moving averages show no clear pattern indicating no obvious trend in the data.

Spatial Structure

The spatial structure within the dataset was evaluated by modeling variograms for each of the facies described in the drill-hole data. Variograms were calculated using the open-source software SGeMS (Stanford Geostatistical Modeling Software). Since the data are categorical, indicator variograms were generated in both the horizontal and vertical directions. Since no significant spatial trends were identified, the data are assumed to be stationary; that is, the likelihood that a particular facies will occur does not change significantly across the basin.

The drill-hole data document geologic facies from land surface to the depth of the drill hole as a nearly continuous record. For this study, the drill-hole data were subsampled every 10 m, and these 10-m subsets were used to construct indicator variograms. Spherical and exponential model variograms were fit by inspection to the vertical experimental variograms (fig. 12a, b). These vertical variograms indicate that each facies is spatially autocorrelated between roughly 200 and 400 m.

Variograms generated in the horizontal direction from the drill hole data did not show strong correlations. This may be due in part to the spatial density of the drill-hole data, which is far less dense in the horizontal direction than in the vertical direction. While vertical variograms are developed from vertical information sampled every 10 m, the development of horizontal variograms is dependent on locally sparse drill-hole data

scattered throughout the study area. Figure 4 shows that about 60 percent of the drill holes are within 1 km of each other, and that only about 20 percent of the drill holes are within 400 m of each other. Thus, any structure smaller than about 1 km will be poorly characterized by the experimental variograms in the horizontal direction. For a more complete data set of the horizontal correlations the surface geologic map was used. The surface geologic map of the alluvium within Yucca Flat (fig. 2; Slate and others, 2000) contains information about spatial continuity of geologic units in the horizontal direction. The geologic map indicates that the Quaternary geologic units are elongated, trending north in the central part of the basin, northwest along the western edge of the basin, and northeast along the eastern edge of the basin; the directions are parallel to the general direction of slope. The Quaternary units on the geologic map show at least 2 km of continuity in the direction of elongation. This suggests that a large range of continuity should be expected in the horizontal direction, and it is assumed for this analysis that alluvial geologic facies in the subsurface have a similar structure to the Quaternary geologic units mapped at the surface. However, the drill-hole data describe geologic facies based primarily on particle size, and thus, the drill-hole data do not directly correlate with the Quaternary units described on the geologic map. Therefore, the geologic map suggests, but does not confirm, greater continuity in the horizontal direction than is observed in the horizontal variograms developed from drill-hole data.

Models of the Alluvium

Overview

The exploratory data analysis provided the framework to define geostatistical models of the subsurface alluvium in Yucca Flat and to compare these models with previous models of the alluvium using the simple measure of bulk hydraulic conductivity. The modeled region is a rectangular volume located within Yucca Flat.

The alluvium within a 5 km by 7 km by 760 m rectangular region beneath the study area, referred to as the subsample study volume (fig. 1), was modeled geostatistically. This volume was chosen to be large enough to accommodate geologic unit and facies changes hundreds to thousands of meters in dimension, to have multiple drill holes to use as hard data for the modeling, and yet to be small enough to make numerical calculations tractable. The subsample study-volume has a relatively large number of drill holes that are relatively evenly spaced, providing ample data to condition the models developed using the various methods, with a north-trending direction of elongation observable in the surface geologic map units (fig. 2).

The homogeneous model of the alluvium, used in the Death Valley regional groundwater flow-system model (Belcher and others, 2004), assumes that the alluvium in Yucca Flat is laterally homogeneous, with a slight decrease in hydraulic conductivity with depth due to compaction. This modeling approach discounts the possibility of preferential paths within the alluvium, excluding facies entirely from the model.

In the model developed by Sweetkind and Drake (2007), which we refer to as the “nearest-neighbor model,” the alluvium is broken out into discrete facies (table 1) based on drill-hole data. The identity of the facies at a given location is estimated by assigning the location the value of the nearest drill-hole data within the same horizontal plane. This

approach is equivalent to interpolating the values using Thiessen (Voronoi) polygons. This simple model of spatial structure is computationally fast and the underlying assumptions are easily understood. However, the spatial structure is dependent solely on the sampling configuration. Densely sampled regions usually generate more complex geological patterns than those that are sparsely sampled because a densely sampled area usually consists of many small Thiessen polygons of different facies. Sparsely sampled areas consist of only a few large Thiessen polygons made up of a small number of facies. An isolated data point, therefore, has a tremendous influence on the modeled spatial structure because a single facie is modeled as covering a very large area. The regions of the study area where the data are least dense have the greatest influence on determining the type of facies present.

For this report the alluvium was modeled using geostatistical methods in order to better characterize the heterogeneous nature of the geology and the hydraulic connectivity within the alluvium. Two general methods were applied: the Sequential Indicator SIMulation method (SISIM) (Deutsch and Journel, 1997), which uses the variogram as a spatial model, and Single Normal Equation SIMulation method (SNESIM) (Strebelle, 2002), which uses the patterns inherent in the surface geologic map as a spatial model. Both methods incorporate spatial structure based on spatial patterns in the data, not on the sampled location. The spatial patterns derived from the data are used to build a mathematical description of spatial correlation among the different facies, which then are used to generate realizations that incorporate observed spatial patterns while simultaneously matching the available drill-hole data. These realizations, generated using the geostatistical models, can be used to estimate the physical properties that define parameters such as bulk hydraulic conductivity, and can be used to describe these parameters statically. The realizations generated using a given geostatistical model, when taken together, provide a distribution of possible geologic properties.

Multiple realizations of the subsurface geology were generated using the SISIM and SNESIM methods and are described in detail in the following sections. Each realization is equally likely, and each fits the available data. A set of 25 realizations was generated for each geostatistical modeling method.

In order to compare the models, the bulk hydraulic conductivity of each model was calculated by assigning individual values of hydraulic conductivity to geologic units and facies and forward modeling the bulk hydraulic conductivity. For the geostatistical models, results for each set of realizations were combined to form an estimate of the distribution of the bulk hydraulic conductivity for the particular geostatistical model. Additionally, the bulk hydraulic conductivity was calculated for the nearest neighbor model. The bulk hydraulic conductivity for the homogeneous model is the same for the entire volume and does not depend on facies, so no calculation is necessary in this case.

Sequential Indicator Simulation Models

The vertical variograms described previously were used as the model of vertical spatial correlation in the SISIM models. Two horizontal variograms were used for the SISIM models, with properties assigned based on the horizontal continuity clearly observed in the geologic map. The drill-hole data generally were too sparse to reliably measure spatial correlation in the horizontal direction for a distance of less than about 1 km. The data were sufficient to measure spatial correlation for greater lags but no strong correlations were discernable. In contrast, the surface geology clearly reveals spatial

correlation on the order of approximately 4 km for the mapped geologic units. This apparent contradiction could indicate a poor correspondence between the units on the surface geologic map and the facies described in the drill-hole data, or that the sampling is not quite dense enough to measure strong spatial correlations. Because horizontal spatial correlation is expected in the subsurface, two models of horizontal spatial correlation were used: a model based on the strong spatial correlation measured from the surface geologic map, and a conservative model, where the horizontal spatial correlation is just below the measurable limit of 1 km. For the first model, referred to as the SISIM-4km model, an anisotropic variogram with a range of 4 km in the direction of elongation (north) and 2 km perpendicular to the direction of elongation was used. This first model is based on the surface geologic map, whose three most abundant geologic units have indicator variograms of approximately these ranges. For the second model, referred to as the SISIM-1km model, an isotropic variogram with a range of 1 km was used. This model assumes that the spatial continuity of the facies is just below the 1-km detectable limit of the horizontal sampling.

Twenty-five SISIM realizations were generated for both of the SISIM models. Each realization represents one possible subsurface unit configuration. Each realization matches the existing drill-hole data and the associated model of spatial structure (the variograms). The resulting geology differs from realization to realization, while still matching all available data. The 25 SISIM-1km realizations tend to have isotropic patches of facies several hundred meters across, as determined by the horizontal variograms with a range of 1 km (figs. 13 and 15). The 25 SISIM-4km realizations tend to have patches of facies elongated north-south, roughly 3 km long, as determined by the horizontal variograms with a range of 4 km in the direction of elongation (figs. 13 and 15).

Single Normal Equation Simulation models

The second geostatistical modeling method used was the single normal equation simulation (SNESIM) method (Strebelle, 2002), which was modified using search tree partitioning (Boucher, 2009). Instead of relying on mathematical functions (for example, variograms) to define the spatial continuity of the geologic units, the SNESIM algorithm defines spatial continuity by measuring the shape and arrangement of geologic units directly from the geologic map (called the training image, in geostatistical parlance). The patterns found in the geologic map are assumed to occur in the region being modeled.

Ideally, in order to model the subsample study volume, a 3D training image would be required. Such an image would need to show alluvial units, similar to those believed to be in the subsurface of Yucca Flat, in three dimensions over an extensive volume. Because such a training image does not exist, the geologic map of Slate and others (1999) was used as the training image for the (two dimensional) lateral continuity. The geologic map was coupled with a vertical variogram to add continuity in the geology in the vertical direction. This new approach, although designed specifically for Yucca Flat, is likely to have a wide range of potential applications.

The lithologic units used for models generated with the SNESIM method are the alluvial units present on the geologic map (Slate and others, 2000), not the facies described in the drill-hole data and used in the SISIM analysis. Six units have been mapped at the surface in the study area: QTa (mixture of Quaternary and Tertiary alluvium), Qai (mixture of Pleistocene alluvium), Qay (mixture of Holocene alluvium),

Qap (active playa deposits), QTc (mixture of Quaternary and Tertiary colluvium), and Qeo (early to middle Pleistocene eolian deposits). The latter two are present only in very minor amounts in Yucca Flat. The hydraulic-conductivity values applied to these units are given in table 2.

Table 2. Hydraulic-conductivity values used for the calculations of bulk hydraulic conductivity for the sub-sample study area. Values are in meters per day. Geologic map units are from Slate and others, 2000.

Facies	High	Medium	Low
gravel	10.4	7.6	4.9
sandy gravel	10.4	7.0	1.3
gravelly sand	6.4	2.7	0.6
sand and minor gravel	4.9	0.6	0.0
sand clay and gravel	0.1	0.1	0.0
coarse sand	10.4	7.6	4.9
fine sand	10.4	5.8	1.3
Geologic map units	0.0	0.0	0.0
QTc	0.1	0.1	0.0
QTa	0.1	0.1	0.0
Qai	4.9	1.2	0.1
Qay	10.4	7.0	1.3
Qp	0.0	0.0	0.0

In order to honor the facies described by the drill-hole data, map units were correlated to drill-hole facies by applying an equal probability to map units that overlapped a single drill-hole facies (table 3). For example, the drill-hole facies “gravelly sand” equates to the map units “Qay” or “Qai”; and any drill-hole interval described as being “gravelly sand” is matched half of the time to geologic map unit “Qay” and half of the time to “Qai”. As stated previously, this correlation is approximate and likely contributes uncertainty to model results.

Table 3. Correlation of geologic map units to facies

Geologic map unit	Drill hole unit
QTc	sand clay and gravel
QTa	sand clay and gravel; sand and minor gravel
Qai	gravelly sand; sand and minor gravel; sand clay and gravel
Qay	sandy gravel; gravel
Qp	sand clay and gravel
Qeo	fine sand; coarse sand

Twenty-five realizations were generated using the SNESIM method, referred to from here on as the SNESIM model. Each realization represents one possible subsurface map unit configuration (figs. 14 and 15). The vertical variograms are used to maintain vertical continuity between geologic units, mimicking the tendency of an alluvial fan depositional environment to remain rather constant over time and only occasionally avulsing and abruptly changing the depositional environment.

Comparing the Models

The effect of geologic heterogeneity on the bulk hydraulic conductivity was evaluated using recently acquired data (Nimmo and others, 2009a; Nimmo and others, 2009b) describing the saturated hydraulic conductivity of geologic units correlative to the geologic units shown on the surface geologic map of Yucca Flat (Menges and others, 2001). The units in Yucca Flat were in turn correlated with the facies descriptions from the drill-hole data. The correlation of geologic units to facies is based primarily on the distribution of particle size in each geologic map unit, as discussed by Nimmo and others (2009a), and secondarily on laboratory measurements of mixtures of coarse and fine sediments (Kolterman and Gorelick, 1995). Although the correlation is approximate and is likely to contribute some uncertainty to the analysis, the hydraulic-conductivity values are based on field measurements of geologic units equivalent to those on the Nevada National Security Site and, therefore, are considered to be the best measurements available.

A range of hydraulic-conductivity values were recorded for each geologic unit (Nimmo and others, 2009b). Similarly, data on the hydraulic conductivity of mixtures of coarse and fine sediment (Kolterman and Gorelick, 1995) show that abrupt changes in hydraulic conductivity can occur across threshold amounts of silt and clay present in the mixture. For this study three hydraulic-conductivity values were considered for each realization, approximated from published graphs (Nimmo and others, 2009b; Kolterman and Gorelick, 1995)—the highest value, the lowest value, and a central value. This resulted in three separate results per realization for the calculation of bulk hydraulic conductivity—high, representing the maximum flow; low, representing the minimum flow; and medium, a central value between the two extremes. The hydraulic-conductivity values used for each geologic unit and facies are given in table 2.

Simulated realizations were input into MODFLOW-2000 (Harbaugh and others, 2000). Hydraulic-conductivity values (table 2) were assigned to each unit within a realization, either high, medium, or low. In a given simulation, all facies were assigned the same group of hydraulic-conductivity values (either all high, all medium, or all low). Assuming saturated flow, MODFLOW was used to forward model the bulk hydraulic conductivity in the vertical (Z) and two primary horizontal (X and Y) directions. Flow was calculated along one direction of the model at a time, confined at the boundaries of the model in the other two primary directions. This resulted in three bulk hydraulic-conductivity values (high, medium, and low), in each of the X, Y, and Z directions, for each realization. The geostatistical models, therefore, have associated with them a distribution of hydraulic conductivity in the X, Y, and Z directions for each of the high, medium, and low values of hydraulic conductivity assigned to the individual facies. Since the nearest neighbor model is a deterministic model, the result is a single estimate of bulk hydraulic conductivity (as opposed to a range that is provided by multiple realizations) for each of the X, Y, and Z directions.

The homogeneous model is not differentiated into facies and, therefore, does not depend on facies hydraulic conductivity. The homogeneous model has a mean bulk hydraulic-conductivity value of 10.8 m/day and a range of 0.00006 to 130 m/day (Belcher, 2004).

Results and Discussion

Bulk hydraulic-conductivity values estimated by the different modeling approaches are shown and compared in figure 16. In almost all cases the resulting bulk hydraulic conductivity is ordered highest to lowest starting with the nearest neighbor model, then the SISIM-4KM model, then the SISIM-1KM model, and finally the SNESIM model. The mean value for the homogeneous model is higher than any of the other models. The variability of the models also is ordered, increasing from the single, deterministic values given by the homogeneous and nearest neighbor model, to moderate variability shown by the SISIM models, to the greatest variability shown by the SNESIM model.

The homogeneous, nearest neighbor, SISIM and SNESIM models generate models that include an increasing amount of geologic information. The homogeneous model assumes no hydrogeologic structure in the alluvium in the subsurface. The nearest neighbor model uses a simple, data-driven interpolation algorithm based solely on the location of the data to generate geologic structure. The SISIM models incorporate the spatial continuity of geologic facies by using the variogram so that the spatial correlation observed between data points is generally maintained. The SNESIM model not only maintains the spatial correlation, but also generally maintains the geologic unit shapes and the spatial organization of the shapes. The SNESIM model, which incorporates vertical correlation through indicator simulation, incorporates the most geologic knowledge of any of the models, and not only matches the surface geology and the drill-hole data, but also maintains geologic unit shape and continuity with depth.

In all cases, the SISIM and SNESIM models generate bulk hydraulic-conductivity values lower than that of the nearest neighbor method. The SISIM models produce bulk hydraulic-conductivity values on the order of 1.5 to 2 times smaller than the bulk hydraulic conductivity predicted by the nearest neighbor model, whereas the SNESIM model produces bulk hydraulic-conductivity values from 2 to 7 times smaller than the value predicted by the nearest neighbor model. The SNESIM model consistently predicts the lowest bulk hydraulic-conductivity values of all of the models. The results indicate that the bulk hydraulic conductivity in Yucca Flat decreases as more information derived from the alluvial sediment package is used to constrain the geologic models. These results imply that, within Yucca Flat, models that do not include the spatial complexity of the alluvial units may tend to over-predict the bulk hydraulic conductivity within the alluvial fill.

The SISIM and SNESIM models offer measures of uncertainty for the predicted values of bulk hydraulic conductivity, lacking in both the homogeneous model and the nearest neighbor model. By generating a range of possible realizations of the subsurface geology for each model of spatial structure, the variation expected for each model of spatial structure was quantified (see histograms in fig. 16). From the graphs it can be seen that the variance of the models is positively correlated with the mean—the lower the mean bulk hydraulic conductivity, the smaller the corresponding standard deviation. Further, in general, the standard deviation of the SISIM models is about 2.5 percent of the mean in the horizontal directions and about 5 percent of the mean in the vertical direction, whereas the standard deviation of the SNESIM models is about 10 percent of the mean in the horizontal directions and about 15 percent of the mean in the vertical

direction. These statistical tendencies indicate a trend towards greater variability in predicted bulk hydraulic conductivity with increased input of geologic information.

One explanation for the results is that as geologic variation is incorporated into the models, the complexity of the system being modeled and the uncertainty of the results becomes more apparent. The SNESIM model best represents the geologic complexity of the alluvium, because it incorporates information about the patterns and proportions of the geologic units expected in the subsurface. When this complexity is incorporated into the calculations of bulk hydraulic conductivity the results show the most variation, implying that models that lack this information are significantly simplified.

In this study, geostatistical models of the alluvium beneath Yucca Flat were compared with existing models. However, it should be noted that units in the geostatistical models were mapped at a finer scale than the existing nearest neighbor model. Additionally, an interpretive correspondence was developed between the drill-hole data and the surface geologic units. While methods certainly play an important role in the modeling, this study ultimately compares the spatial distributions resulting from the different models, not the methods.

Summary of Results

This study provides an alternative set of 3D models of the alluvium for a subregion in Yucca Flat. Models differ in their predicted bulk hydraulic-conductivity values from that predicted by the previous nearest neighbor and homogeneous models. These new geostatistical models of the alluvium in Yucca Flat incorporate more information about the dimensions, shape, and continuity of the alluvial units in the subsurface than previous deterministic models. These geostatistical models can provide measures of uncertainty for model parameters.

The values for bulk hydraulic conductivity within the alluvial units in Yucca Flat predicted by the geostatistical models are increasingly lower than those predicted by earlier models by as much as a factor of seven. Generally, the predicted value for bulk hydraulic conductivity decreases with added geologic information.

The uncertainty in the predicted value of hydraulic conductivity associated with the geostatistical models varies with the predicted mean value. The uncertainty increases as the amount of geologic information used to create the model increases. The model that incorporates the greatest amount of information about the alluvial geology, the SNESIM model, has the largest uncertainty associated with its predicted values of hydraulic conductivity. These parameter differences between models may have a significant effect on any subsequent flow and transport modeling.

Acknowledgments

This work was made possible by the DOE DE-AI52-07NA28100. The manuscript was greatly improved by the comments of the reviewers R.J. Lacznik and D.R. Bedford. The authors would like to thank all involved for helping to make this work possible.

References

- Belcher, W.R., ed., 2004, Death Valley regional ground-water flow system, Nevada and California—Hydrogeologic framework and transient ground-water flow model: U.S. Geological Survey Scientific Investigations Report 2004-5205, 408 p.
- Boucher, A., 2009, Considering complex training images with search tree partitioning: *Computers & Geosciences*, v. 35, no. 6, p. 1151-1158.
- Carr, W.J., 1984, Regional structural setting of Yucca Mountain, southeastern Nevada, and late Cenozoic rates of tectonic activity in part of the southwestern Great Basin, Nevada and California: U.S. Geological Survey Open-File Report 84-854, 114 p.
- Cleveland, W.S., 1979, Robust locally weighted regression and smoothing scatterplots: *Journal of the American Statistical Association*, v. 74, no. 368, p. 829-836.
- Cole, J.C., and Dickinson, W.R., 1987, Breakup of an allochthonous slab; origin of the Yucca Flat Basin, Nevada Test Site: *Geological Society of America —Abstracts with Programs*, v. 19, no. 7, p. 1.
- Cole, J.C., Harris, A.G., and Wahl, R.R., 1997, Sub-crop geologic map of pre-Tertiary rocks in the Yucca Flat and northern Frenchman Flat areas, Nevada Test Site, Nevada: U.S. Geological Survey Open-File Report 97-678, 24 p.
- Deutsch, C.V., and Journel, A.G., 1997, *GSLIB: Geostatistical Software Library and User's Guide*: Oxford University Press, 384 p.
- Guertal, W.R., Flint, A.L., Hofmann, L.L., and Hudson, D.B., 1994, Characterization of a desert soil sequence at Yucca Mountain, NV: *High-Level Radioactive Waste Management, Proceedings of the Fifth Annual International Conference*, May 22-26, Las Vegas, Nevada, American Nuclear Society, LaGrange Park, Ill., p. 2755-2761.
- Harbaugh, A.W., Banta, E.R., Hill, M.C., and McDonald, M.G., 2000, MODFLOW-2000, the U.S. Geological Survey modular ground-water model—User guide to modularization concepts and the Ground-Water Flow Process: U.S. Geological Survey Open-File Report 00-92, 121 p.
- Klise, K.A., McKenna, S.A., Tidwell, V.C., Lane, J.W., Weissmann, G.S., Wawrzyniec, T.F., and Nichols, E.M., 2009, Causal factors of non-Fickian dispersion explored through measures of aquifer connectivity: *Proceedings of IAMG, Annual Conference of the International Association for Mathematical Geology*, Stanford University, August 23-27, p. 10.
- Kolterman, C.E., and Gorelick, S.M., 1995, Fractional packing model for hydraulic conductivity derived from sediment mixtures: *Water Resources Research*, v. 31, no. 12, p. 3283-3297.
- Laurini, R., and Thompson, D., 1992, *Fundamentals of Spatial Information Systems*: San Diego, Academic Press Inc.
- Menges, C.M., Taylor, E.M., Workman, J.B., and Jayko, A.S., 2001, Regional surficial-deposit mapping in the Death Valley area of California and Nevada in support of ground-water modeling, in Machette, M.N., Johnson, M.L., and Slate, J.L., eds., *Quaternary and late Pliocene geology of the Death Valley region: Recent observations on tectonics, stratigraphy, and lake cycle—Pacific Cell-Friends of the Pleistocene Field-trip Guidebook*: U.S. Geological Survey Open-File Report 01-51, p. H151-H166.

- Nimmo, J.R., Perkins, K.S., Schmidt, K.M., Miller, D.M., Stock, J.D., Singha, K., Andraski, B.J., and Munoz-Carpena, R., 2009a, Hydrologic characterization of Desert soils with varying degrees of pedogenesis; 1, Field experiments evaluating plant-relevant soil water behavior: *Vadose Zone Journal*, v. 8, no. 2, p. 480-495.
- Nimmo, J.R., Schmidt, K.M., Perkins, K.S., and Stock, J.D., 2009b, Rapid measurement of field-saturated hydraulic conductivity for areal characterization: *Vadose Zone Journal*, v. 8, no. 1, p. 142-149.
- Ponce, D.A., 1997, Gravity data of Nevada: U.S. Geological Survey Digital Data Series Report 42, 28 p., CD-ROM.
- Sawyer, D.A., Fleck, R.J., Lanphere, M.A., Warren, R.G., Broxton, D.E., and Hudson, M.R., 1994, Episodic caldera volcanism in the Miocene southwestern Nevada volcanic field; revised stratigraphic framework, (super 40) Ar/ (super 39) Ar geochronology, and implications for magmatism and extension: *Geological Society of America Bulletin*, v. 106, no. 10, p. 1304-1318.
- Slate, J.L., Berry, M.E., Rowley, P.D., Fridrich, C.J., Morgan, K.S., Workman, J.B., Young, O.D., Dixon, G.L., Williams, V.S., McKee, E.H., Ponce, D.A., Hildenbrand, T.G., Swadley, W.C., Lundstrom, S.C., Ekren, E.B., Warren, R.G., Cole, J.C., Fleck, R.J., Lanphere, M.A., Sawyer, D.A., Minor, S.A., Grunwald, D.J., Laczniak, R.J., Menges, C.M., Yount, J.C., and Jayko, A.S., 2000, Digital geologic map of the Nevada Test Site and vicinity, Nye, Lincoln, and Clark Counties, Nevada, and Inyo County, California: U.S. Geological Survey Open-File Report 99-554A, 53 p., scale 1:120,000.
- Strebelle, S., 2002, Conditional simulation of complex geological structures using multiple-point statistics: *Mathematical Geology*, v. 34, no. 1, p. 1-21.
- Sweetkind, D.S., and Drake, R.M. II, 2007, Geologic characterization of young alluvial basin-fill deposits from drill-hole data in Yucca Flat, Nye County, Nevada: U.S. Geological Survey Scientific Investigations Report 2007-5062, 17 p.

Figures

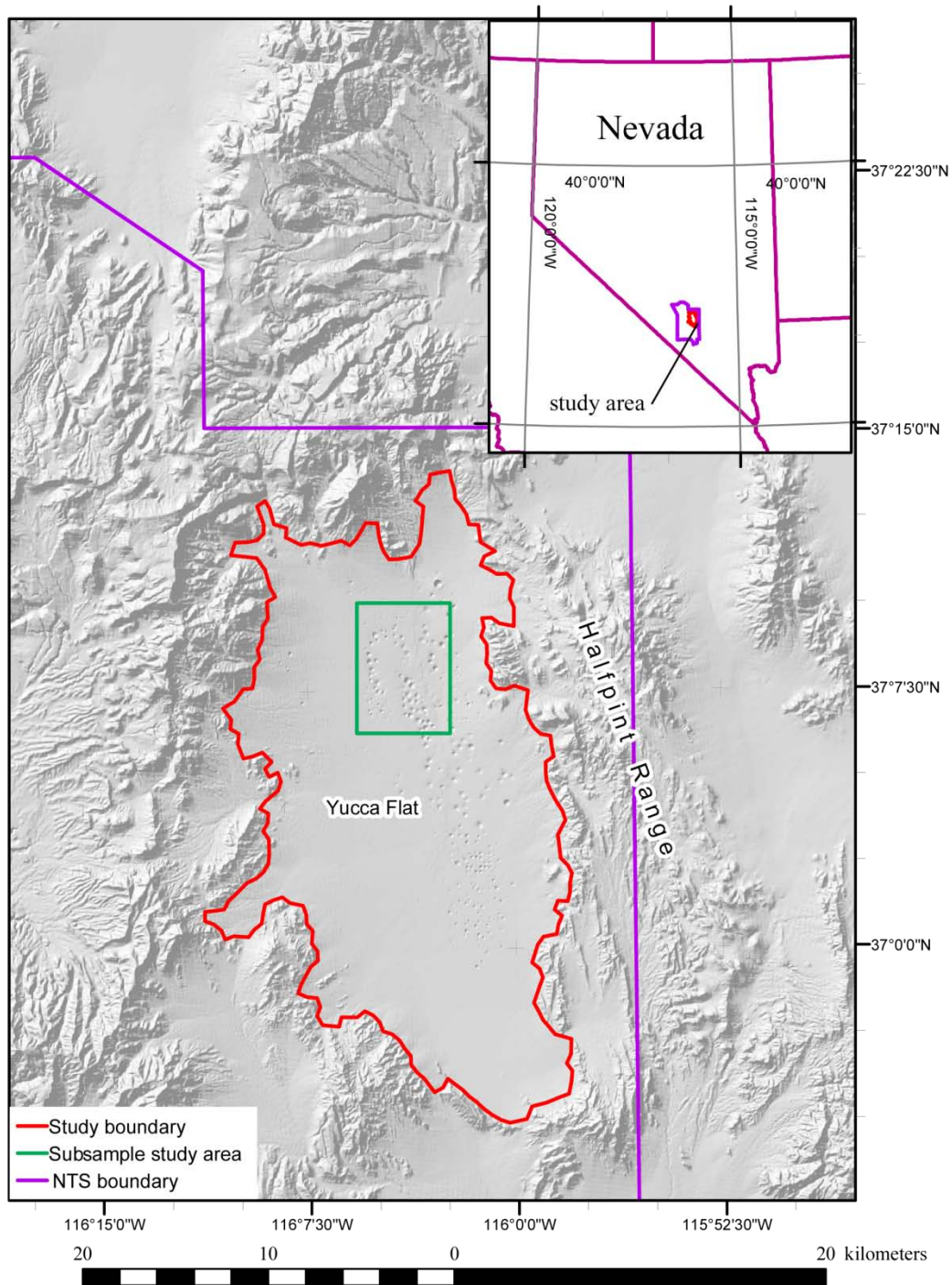


Figure 1. Map of study area, smaller subsample study area, and major place names, Yucca Flat, Nevada. Shaded relief map compiled from merged 30 m USGS DEMs.

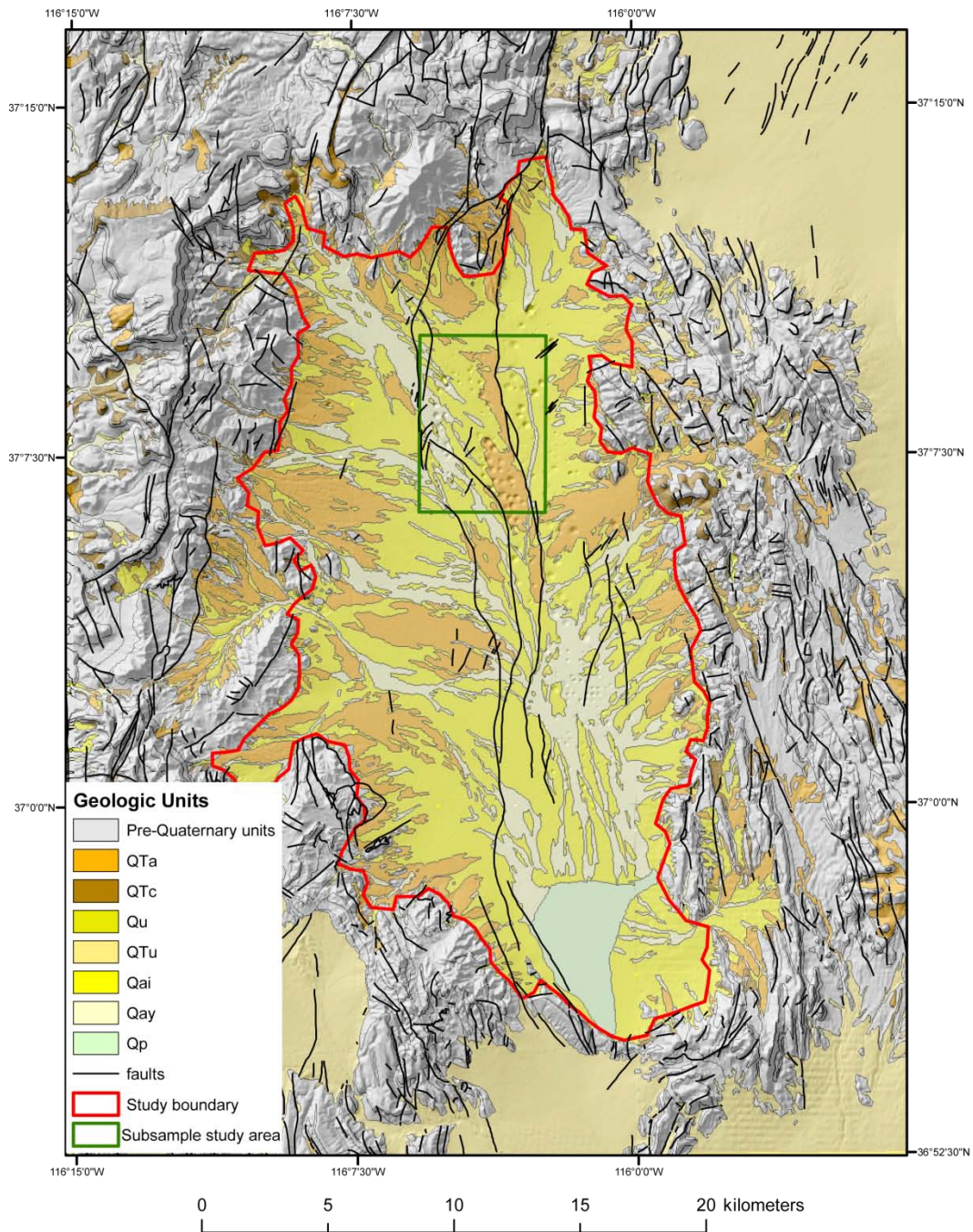


Figure 2. Quaternary geology of Yucca Flat Basin, (Slate and others, 2000), displayed on shaded relief map (merged USGS 30 meter DEMs). Refer to Slate and others (2000) for unit explanations.

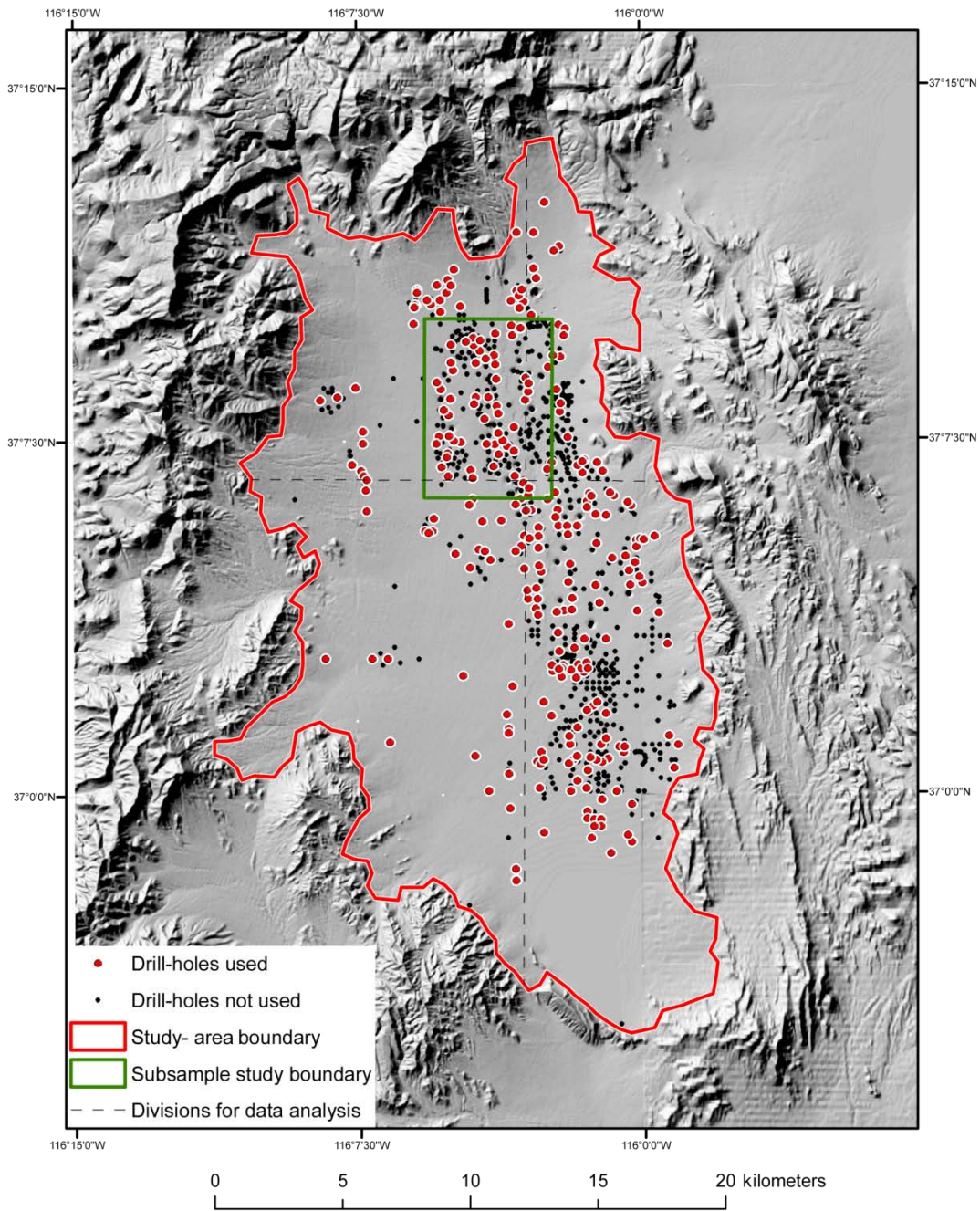


Figure 3. Drill holes penetrating alluvium in Yucca Flat Basin, Nevada. Larger red dots show drill holes used to characterize Yucca Flat alluvium. Smaller black dots show drill holes not used. Dashed lines divide the basin into four quadrants for analysis, as discussed in the Exploratory Data Analysis section.

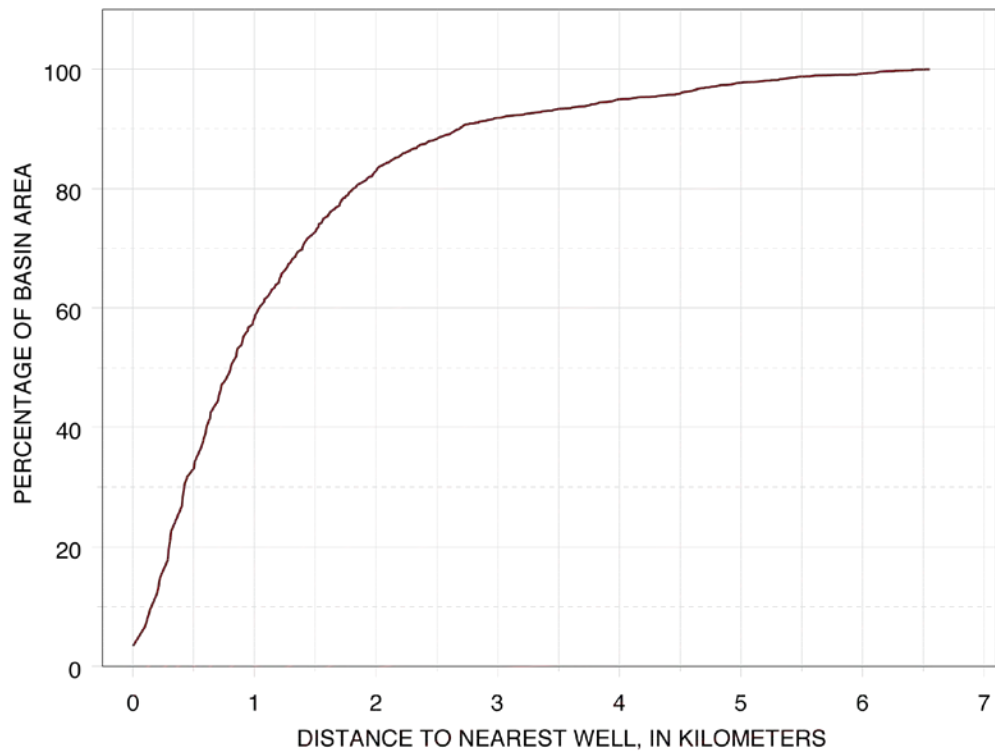


Figure 4. Cumulative percentage of area in the basin with a drill hole at or closer than the specified distance.

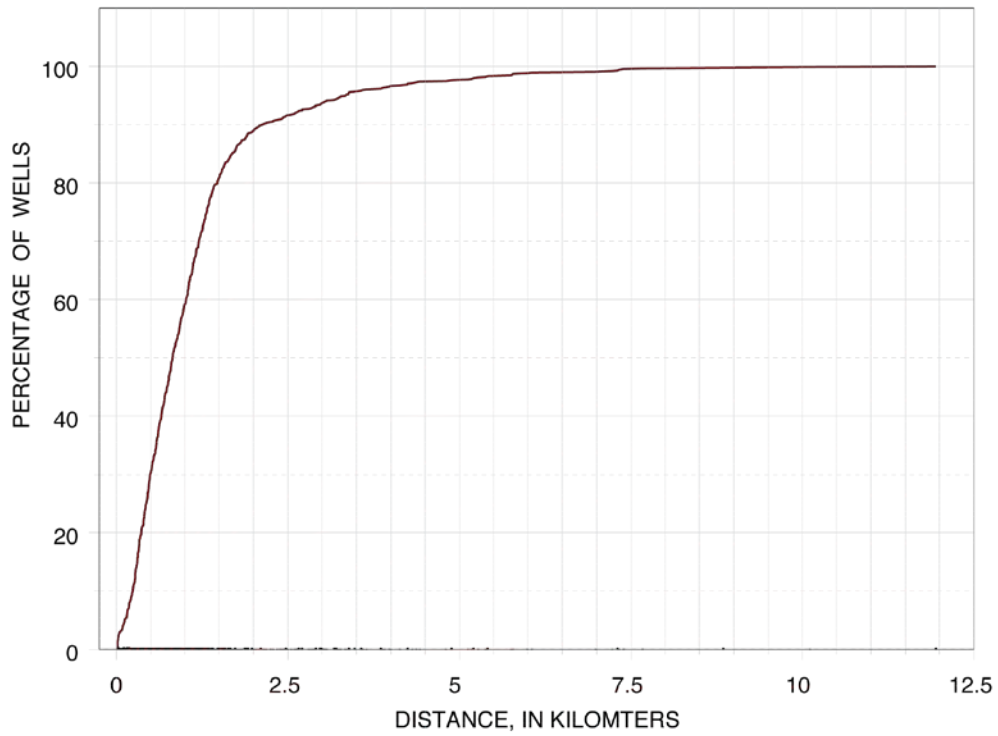


Figure 5. The cumulative distribution of the natural neighbor distance between drill holes used in this analysis. The graph estimates the horizontal clustering of drill-hole sampling.

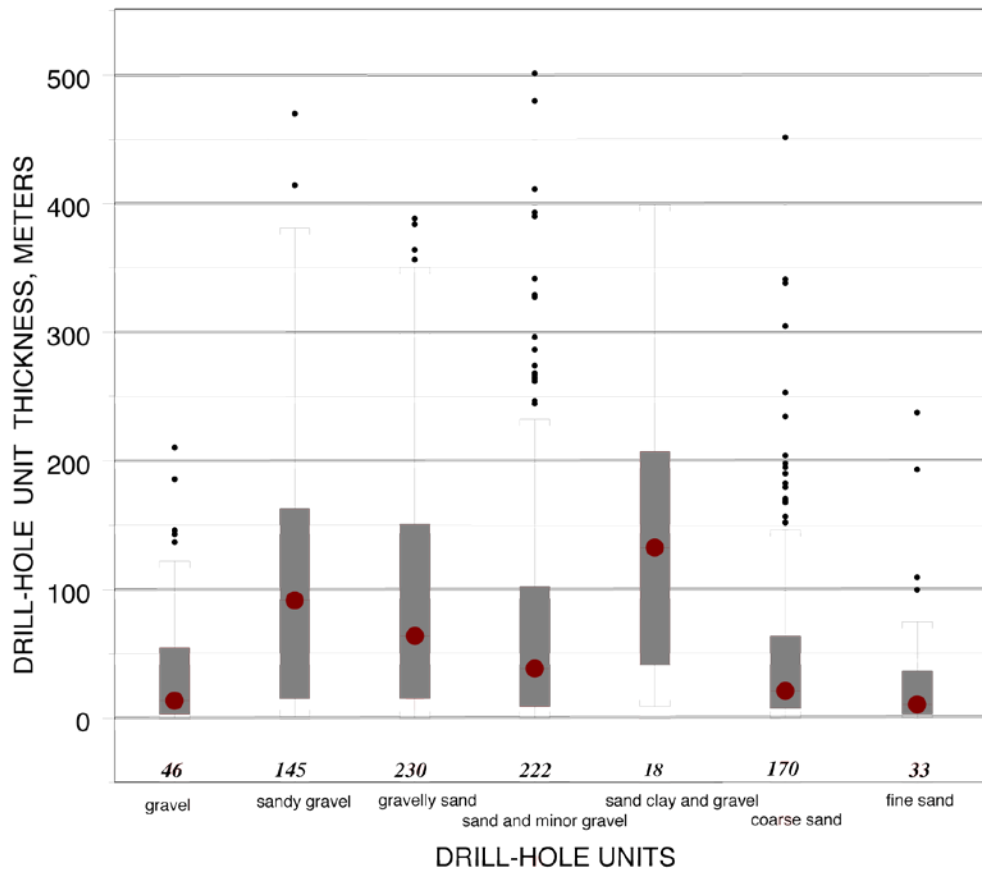


Figure 6. Thickness distributions for the major drill-hole facies in the alluvium of Yucca Flat Basin. Numbers along the X-axis are the number of samples. For the box plot, red dot represents the median, grey box the hinges (median of the upper and lower half of the data), black dots outliers beyond the span, and whiskers the span ($1.5 * [\text{upper hinge} - \text{lower hinge}]$).

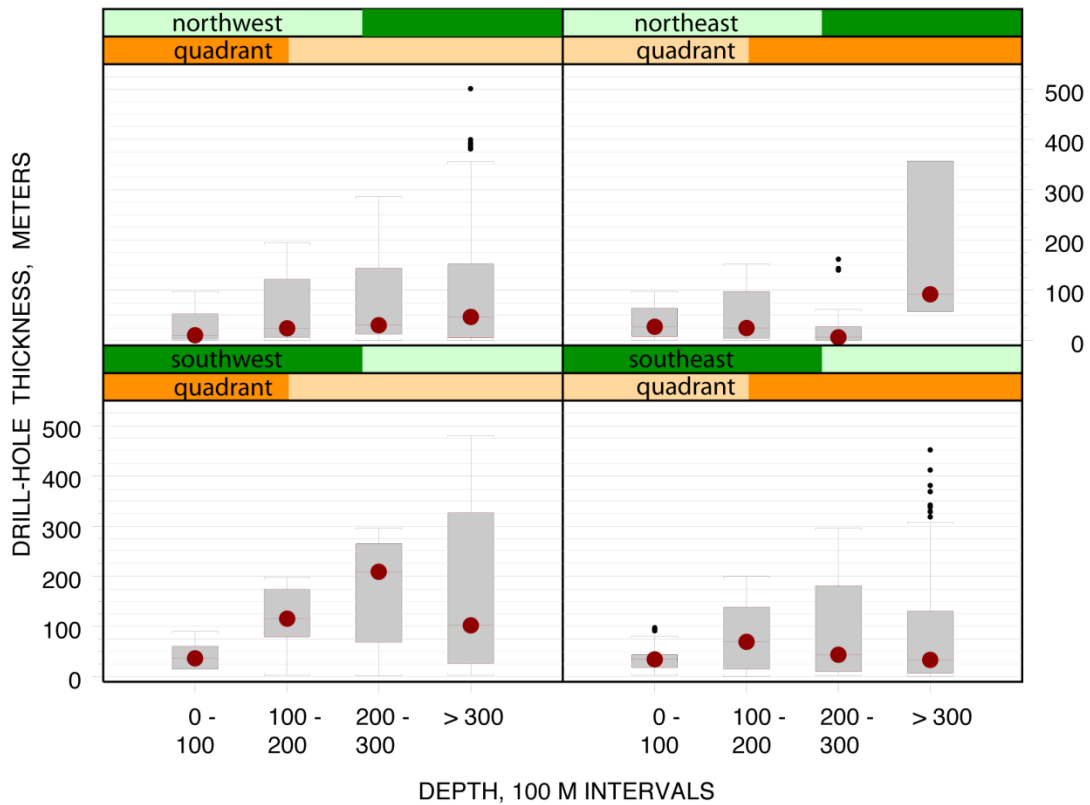


Figure 7. Box plots of unit thickness subset by the depth of the bottom of the unit, for each basin quadrant (shown in figure 3). Panels are consistent with map direction, that is, upper left panel shows the data for the northwest quadrant. Dark colors in panel headings indicate location of quadrant: orange for west (left) or east (right), green for south (left) or north (right). See figure 6 for explanation of box plots.

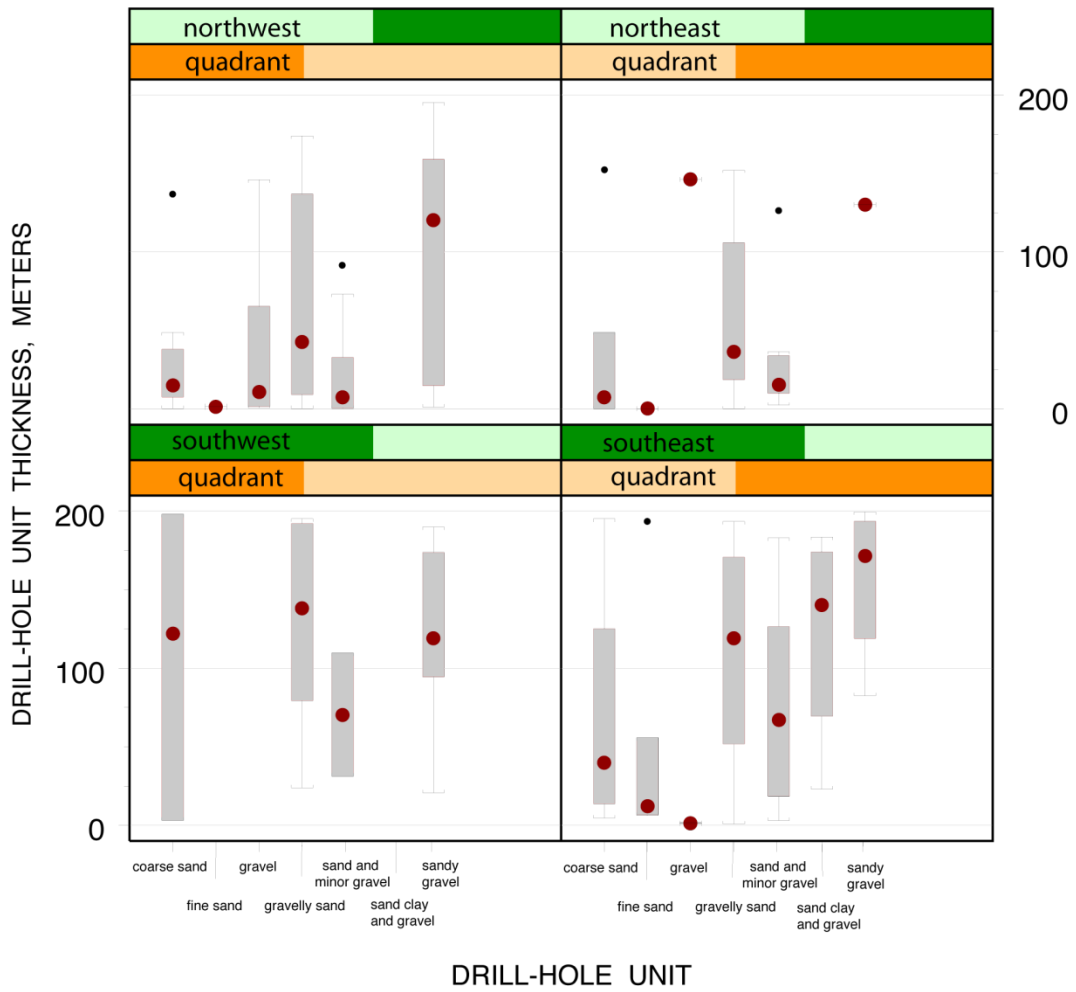


Figure 8. Box plots of drill-hole unit thickness subset by drill-hole unit and by basin quadrant (shown in figure 3), for units whose bottom depth is between 100 and 200 m. Dark colors in panel headings indicate location of quadrant: orange for west (left) or east (right), green for south (left) or north (right). See figure 6 for explanation of box plots.

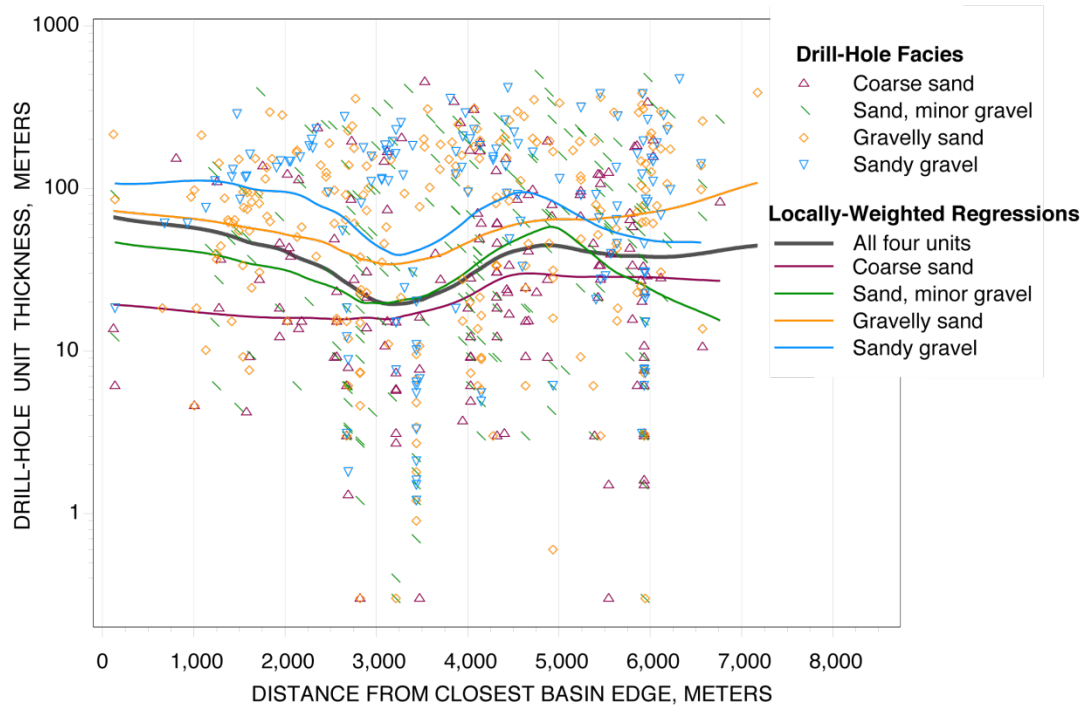


Figure 9. Scatter plot of drill-hole unit thickness (log scale) versus distance from the closest basin edge for the four most abundant drill-hole units. Lines are locally-weighted regression fits for each unit.

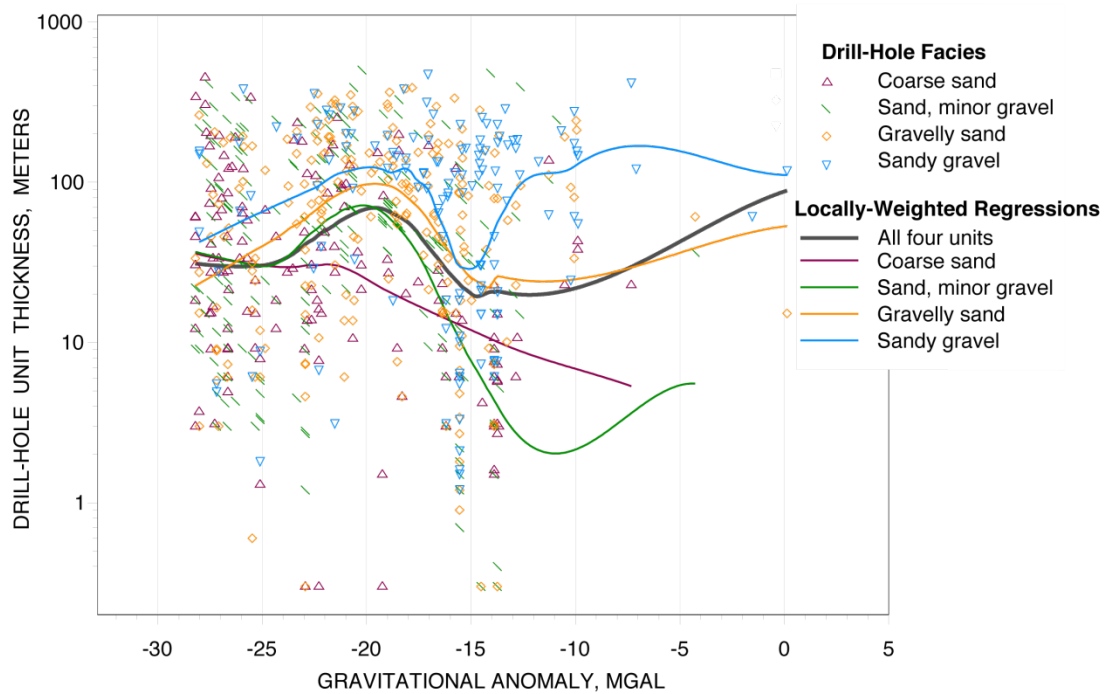


Figure 10. Drill-hole unit thickness (log scale) versus gravitational anomaly. Lines are locally-weighted regression fits for each unit.

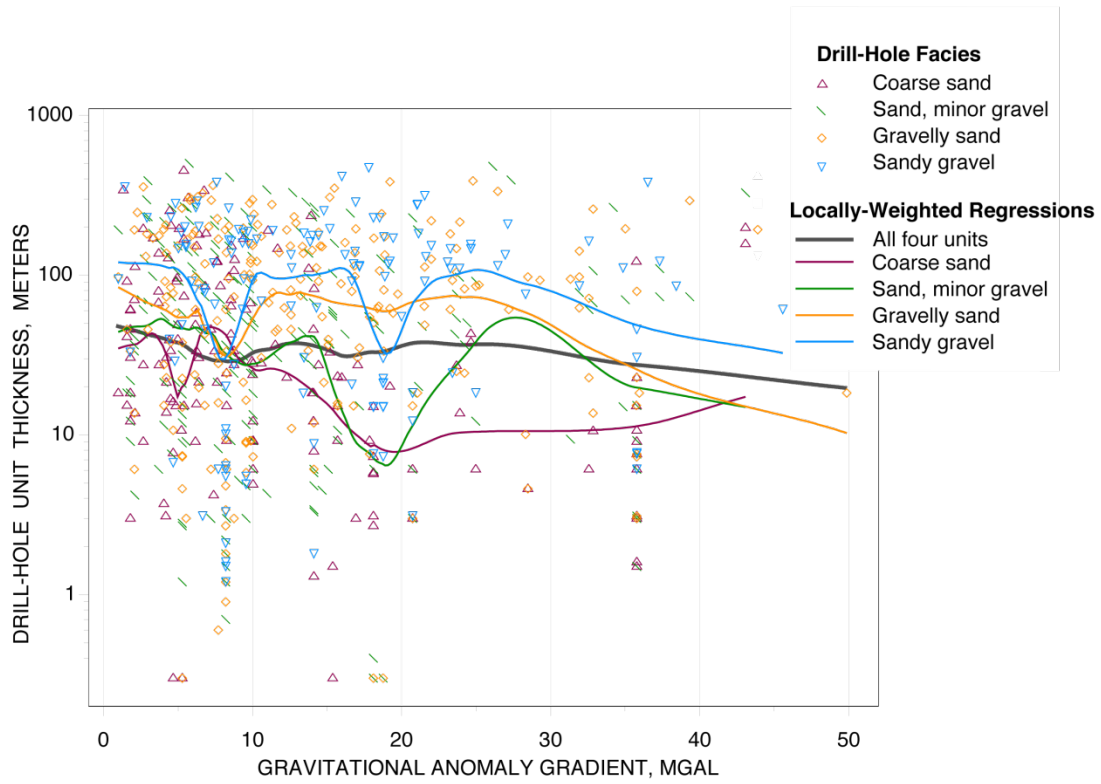


Figure 11. Scatter plot of unit thickness (log scale) versus gravitational gradient for the four most abundant drill-hole units. Lines are locally-weighted regression fits for each unit.

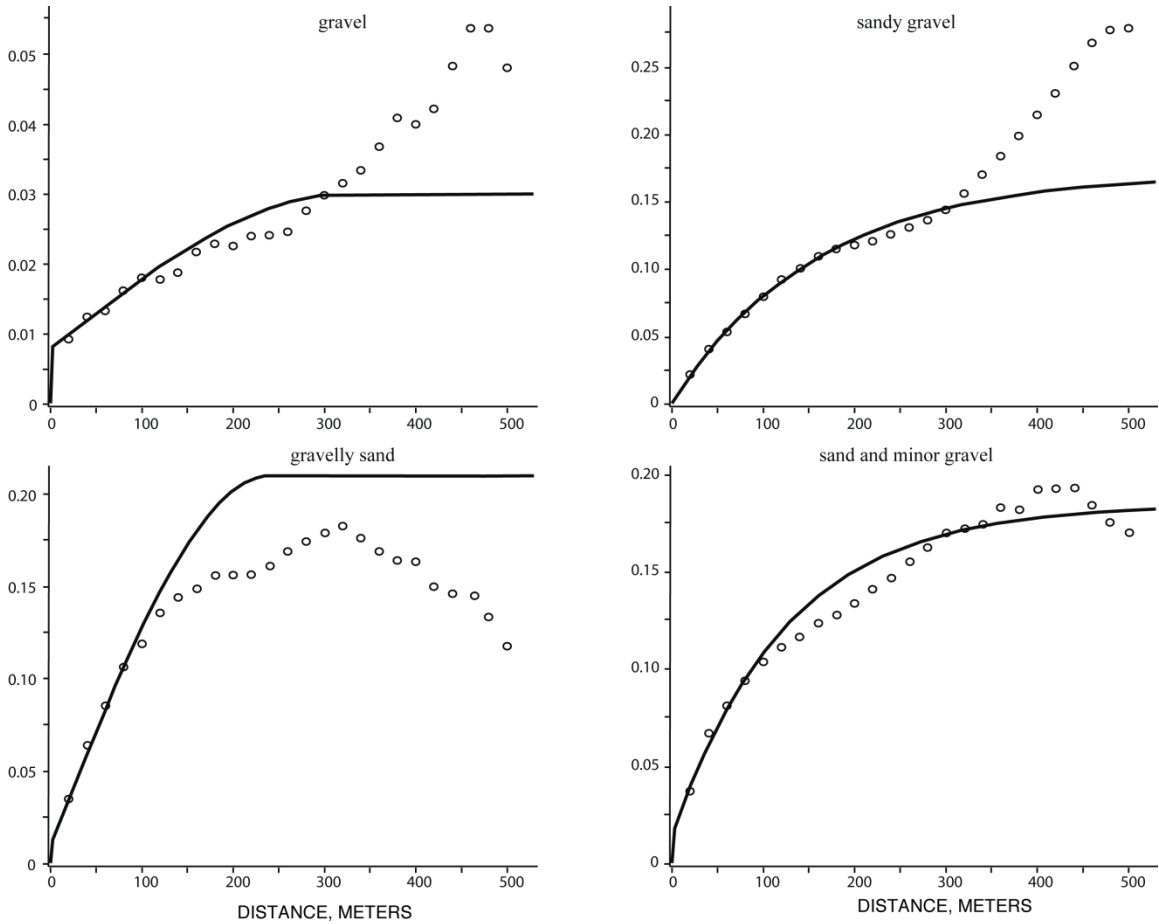


Figure 12a. Vertical indicator variograms used for the sequential indicator simulation model. This page —gravel, sandy gravel, gravelly sand, sand and minor gravel.

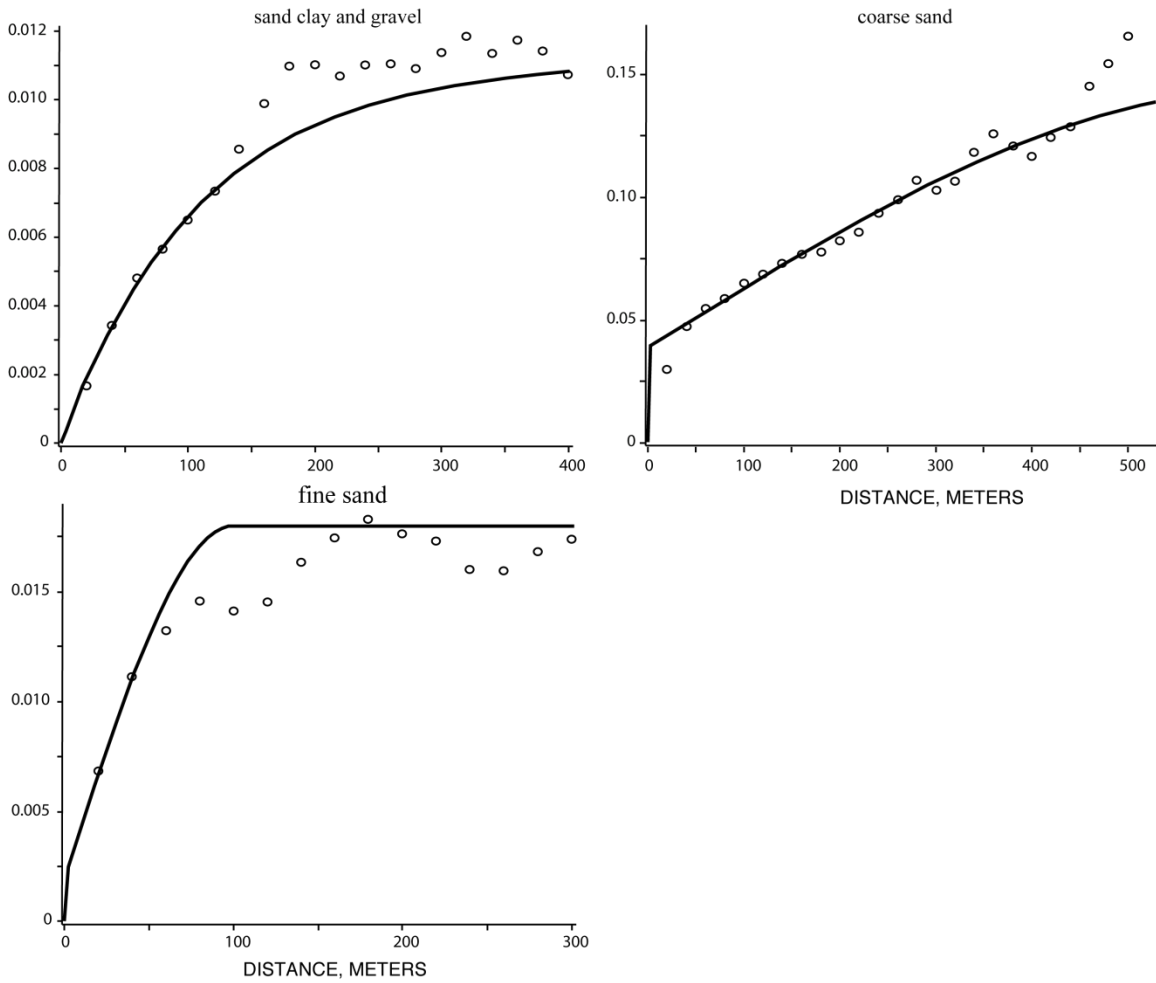


Figure 12b. Vertical indicator variograms used for the sequential indicator simulation model. This page —sand clay and gravel, coarse sand, fine sand.

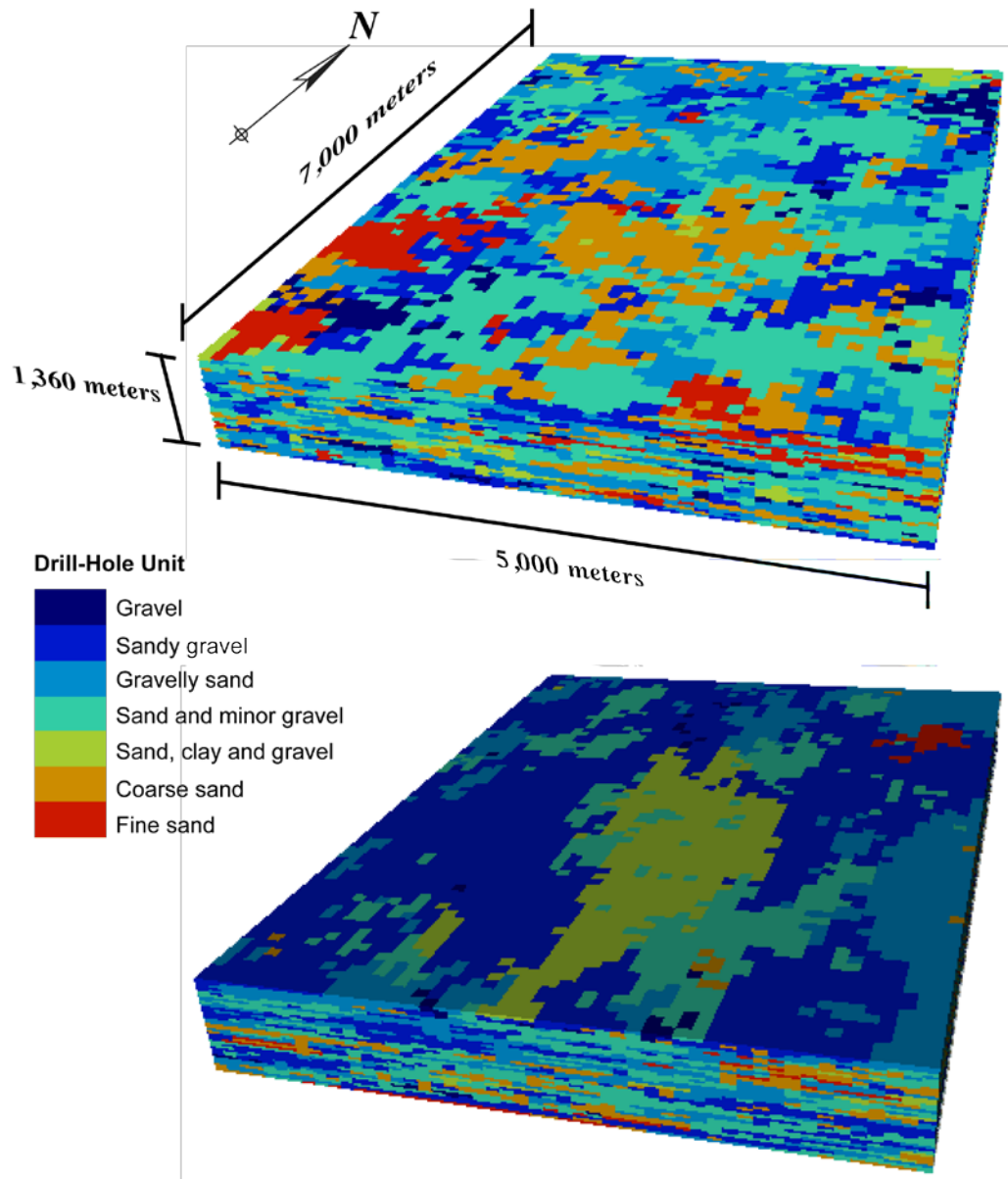


Figure 13. Example realization from each model of spatial structure used to generate the 25 SISIM realizations; (top) SISIM-1KM; (bottom) SISIM-4KM.

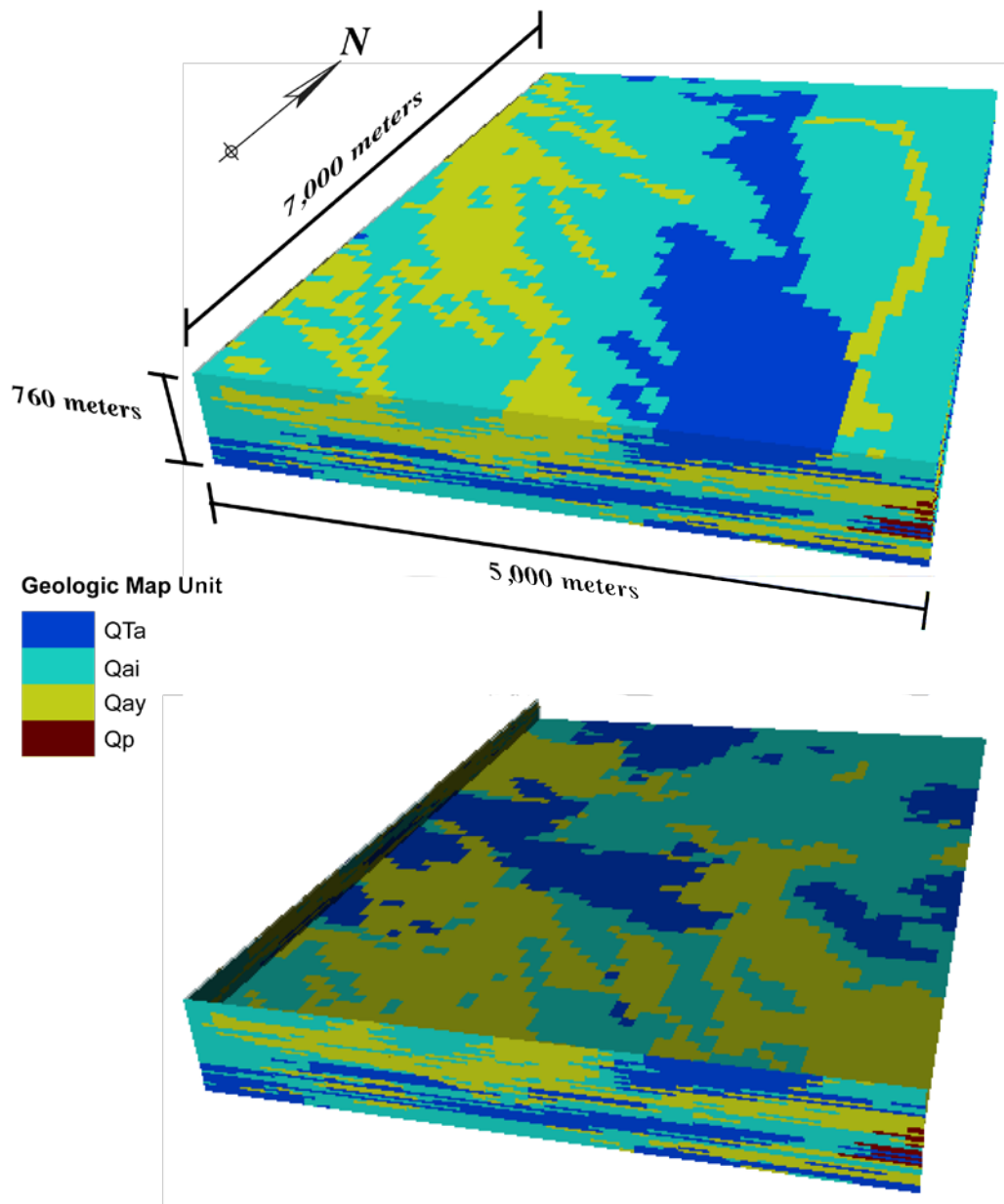


Figure 14 One hybrid SNESIM realization, which uses the geologic map and the vertical variograms to model the spatial structure. Note that the surface (block view, top) always matches the observations from the geologic map (surface data), while the subsurface (sliced view, bottom) will change according to the realization. Four of the six geologic map units present in the realizations are visible in these two block views.

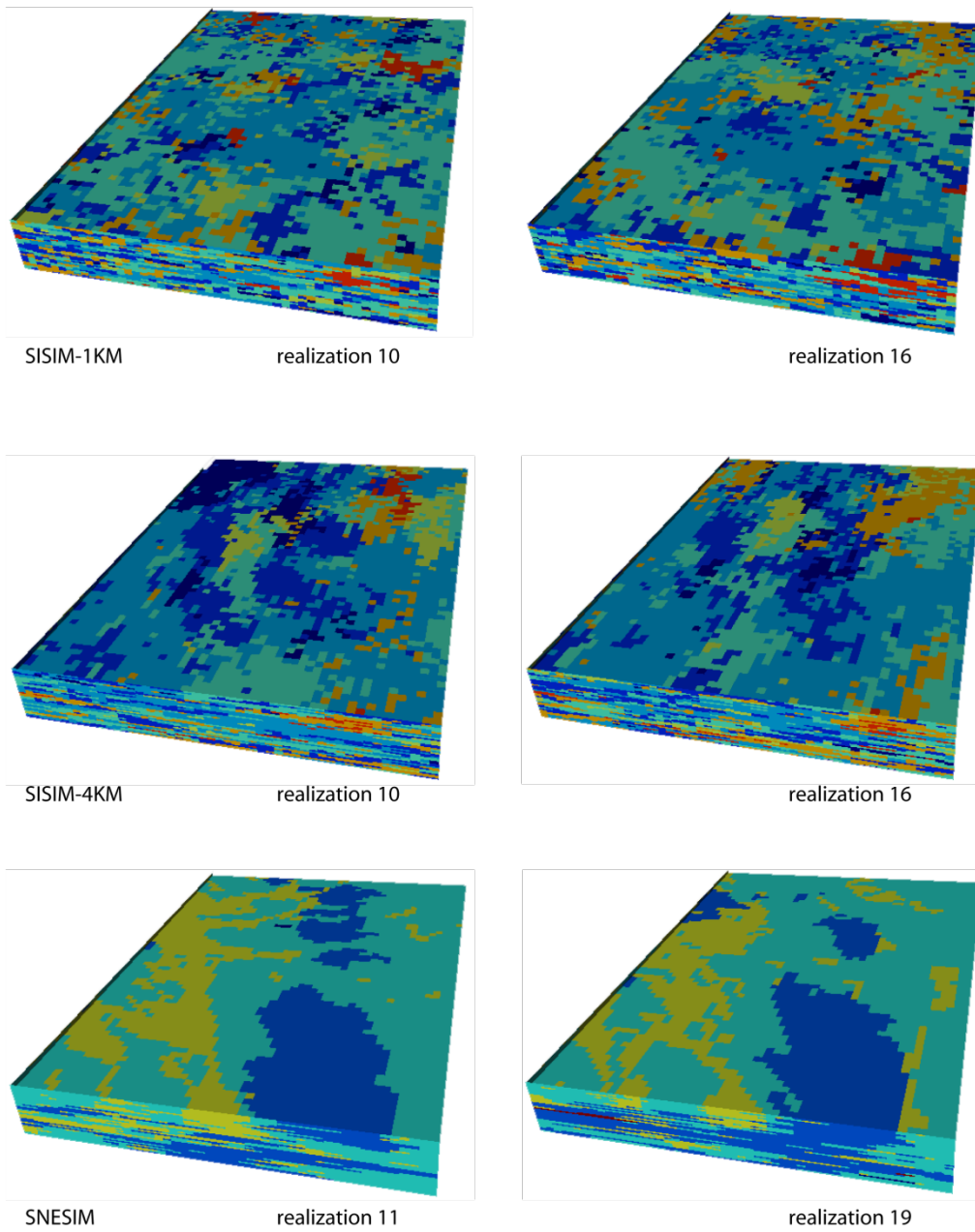


Figure 15. Two arbitrary realizations from each of the geostatistical models: SISIM-1KM, SISIM-4KM, and SNESIM. Dimensions of the volume, direction of north, and colors used for facies and geologic units are identical to those shown on figures 13 and 14.

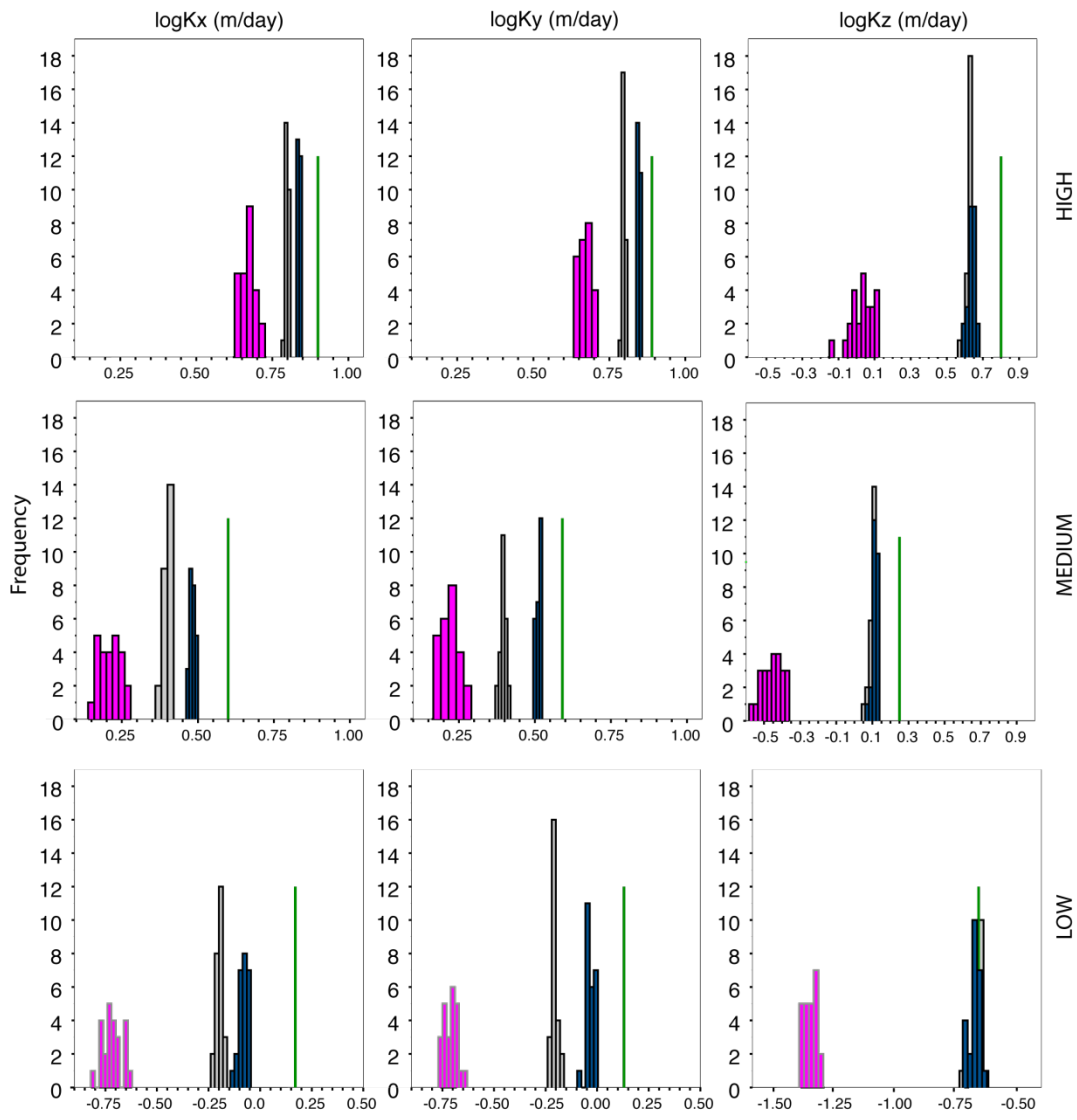


Figure 16. Histograms of the log of the bulk hydraulic-conductivity values (measured in meters/day) in the X, Y, and Z directions (left to right columns, respectively) for the high, medium, and low (top to bottom rows, respectively) values of hydraulic conductivity. Bars are colored according to the model: SNESIM (purple), SISIM-1KM (grey), SISIM-4KM (dark blue), and nearest neighbor (green). Note horizontal scale on the last row is shifted with respect to rows above.